

Frédérique Tête-Favier,^a David Cobessi,^a Gordon A. Leonard,^b Saïd Azza,^c François Talfournier,^c Sandrine Boschi-Muller,^c Guy Branlant^c and André Aubry^{a*}

^aLaboratoire de Cristallographie et de Modélisation des Matériaux Minéraux et Biologiques, Groupe Biocristallographie, ESA 7036, BP 239, F-54506 Vandoeuvre-lès-Nancy CEDEX, France, ^bJoint Structural Biology Group, ESRF, BP220, F-38043 Grenoble CEDEX, France, and ^cLaboratoire de Maturation des ARN et Enzymologie Moléculaire, UMR 7567, BP 239, F-54506 Vandoeuvre-lès-Nancy CEDEX, France

Correspondence e-mail:
aubry@lcm3b.u-nancy.fr

Crystallization and preliminary X-ray diffraction studies of the peptide methionine sulfoxide reductase from *Escherichia coli*

Peptide methionine sulfoxide reductase mediates the reduction of protein sulfoxide methionyl residues back to methionines and could thus be implicated in the antioxidant defence of organisms. Hexagonal crystals of the *Escherichia coli* enzyme (MsrA) were obtained by the hanging-drop vapour-diffusion technique. They belong to space group $P6_522$, with unit-cell parameters $a = b = 102.5$, $c = 292.3$ Å, $\gamma = 120^\circ$. A native data set was collected at 1.9 Å resolution. Crystals of selenomethionine-substituted MsrA were also grown under the same crystallization conditions. A three-wavelength MAD experiment has led to the elucidation of the positions of the Se atoms and should result in a full structure determination.

Received 22 May 2000
Accepted 30 June 2000

1. Introduction

Numerous active oxidative species such as hydroxyl radicals (OH[•]), superoxide anions (O₂^{•-}), hydrogen peroxide (H₂O₂) or hypochlorite ions (OCI⁻) are naturally produced in biological systems. Their high reactivity can cause cellular damage, which increases with organism ageing. In particular, peptide methionyl residues are very sensitive to oxidative stress as they easily form methionine sulfoxides (Vogt, 1995). While some surface methionines are oxidized with only slight modification of protein properties, leading these to be proposed as antioxidants (Levine *et al.*, 1999), there are many cases where methionine oxidation has a large effect on the function of proteins. Enzymatic activity can be lost by oxidation directly occurring in the active site. Moreover, secondary structures can also be altered (Sigalov & Stern, 1998; Sun *et al.*, 1999). To lessen the risk of cellular dysfunction as a result of this, many organisms possess an enzyme called peptide methionine sulfoxide reductase (PMSR; E.C. 1.8.4.6) which reduces peptide methionine sulfoxides back to peptide methionines and restores protein function. It can thus be proposed that the presence of PMSR is crucial in these organisms as a result of its ability to reduce oxidized methionines in proteins. Other roles have also been proposed for PMSR. It could be an antioxidant *in vivo* as it provides cells with resistance to oxidative stress (Moskovitz *et al.*, 1997, 1999; El Hassouni *et al.*, 1999) or it could act as a regulator of processes which involve methionine oxidation (Sun *et al.*, 1999; Ciorba *et al.*, 1997). Results of site-directed mutagenesis, biochemical and biophysical studies have recently been published (Lowther *et al.*, 2000; Moskovitz *et al.*, 2000). They revealed several

conserved amino acids that could play a role in the active site of PMSRs. A catalytic mechanism in which three cysteine residues and a thioredoxin regeneration system could be involved was proposed (Lowther *et al.*, 2000).

More than 40 PMSR sequences are known to date. Regarding those biochemically characterized, it appears that active PMSRs are approximately 200 amino acids in length. The *E. coli* PMSR named MsrA (Brot *et al.*, 1981), with 211 amino acids (23.2 kDa), is a good representative of PMSR sequences. To deepen the knowledge of these important enzymes involved in cellular detoxification and regulation, the X-ray determination of the MsrA three-dimensional structure has been undertaken. As PMSRs show no significant similarity to other proteins, the use of selenomethionine-substituted MsrA ([SeMet]-MsrA) and multi-wavelength anomalous diffraction phasing measurements (MAD) was chosen as a strategy to solve the structure. Here, we describe the preliminary studies (crystallization and data collection) of MsrA and [SeMet]-MsrA.

2. Materials and methods

2.1. MsrA and [SeMet]-MsrA production and purification

E. coli MsrA was produced and purified as described by Boschi-Muller *et al.* (in preparation). *E. coli* strain B834(DE3) containing plasmid pETMsrA (pET24a plasmid containing the MsrA coding sequence under the control of the T7 promoter) was cultured as described by Ramakrishnan *et al.* (1993) and

Table 1
Optimal MsrA crystallization conditions.

Three different conditions obtained from the initial screens gave the same tetragonal crystals and are listed here. The number of molecules per asymmetric unit, V_m , and solvent content are derived from Matthews' formula (Matthews, 1968). As tetragonal and orthorhombic crystals have a possible number of molecules varying over a large range, the values given here are restricted to a mean solvent content of 50%. For hexagonal crystals, V_m values (solvent contents) ranging from 1.64 to 4.92 Å³ Da⁻¹ (75–25%) were considered acceptable.

Crystal form	Tetragonal	Orthorhombic	Hexagonal
Protein concentration (mg ml ⁻¹)	(i) 30; (ii) 20; (iii) 15	40	40
Precipitant solution	(i) 1.9 M ammonium phosphate, 100 mM Tris pH 8.2; (ii) 1.4 M lithium sulfate, 100 mM HEPES pH 7.4; (iii) 0.5 M ammonium sulfate, 0.85 M lithium sulfate	20% PEG 8000, 0.35 M ammonium sulfate, 100 mM cacodylate pH 6.0	20% PEG 8000, 0.35 M ammonium sulfate, 100 mM cacodylate pH 7.0
Maximal size (µm)	800 × 600 × 600	1000 × 400 × 150	1000 × 200 × 200
Waiting period	(i) 10 d; (ii) 1 week; (iii) 1 d	4 weeks	6 weeks
Cryoprotectant solution	Successive soaking in 5/10/15/17.5% ethylene glycol mixed with precipitant	Fast soaking in 15% glycerol mixed with precipitant	Fast soaking in 15% glycerol mixed with precipitant
Unit-cell parameters (Å, °)	$a = b = 176.8, c = 143.7$	$a = 104, b = 182, c = 291$	$a = b = 102.5, c = 292.3,$ $\gamma = 120$
Space group	$I4_1$	Primitive lattice	$P6_322$
Molecules per asymmetric unit	10	24	2–5
V_m (Å ³ Da ⁻¹) (solvent content, %)	2.46 (50)	2.46 (50)	1.91–4.78 (74–23)
Useful diffraction limit (Å)	3.5	3.5	1.9

Table 2
Statistics of X-ray diffraction data collection for the MsrA hexagonal crystals.

Values in parentheses refer to data in the highest resolution shell.

Wavelength (Å)	0.9797 (ESRF, BM30)
Temperature (K)	100
Resolution (Å)	30–1.9 (1.97–1.90)
No. of measured reflections	291810
No. of independent reflections	64402
Completeness (%)	88.9 (65.6)
R_{sym} (%)	3.5 (23.5)
$\langle I \rangle / \langle \sigma \rangle$	21.0 (4.0)

was used as a source of [SeMet]-MsrA. Purification of [SeMet]-MsrA was performed following a procedure similar to that described for MsrA. The presence of a unique protein population was verified by electrospray mass analysis and the molecular mass observed was in good agreement with a full substitution of the six methionine residues by selenomethionines in [SeMet]-MsrA.

2.2. Crystallization

Purified MsrA was dialysed in 50 mM Tris-HCl pH 8.0 buffer containing 2 mM EDTA, 10 mM DTT. Crystallization was achieved using the hanging-drop vapour-diffusion method in Linbro multiwell tissue-culture plates. The search for initial crystallization conditions was performed by sparse-matrix sampling using the screens of

Jancarik & Kim (1991) and Cudney *et al.* (1994) at 277 and 293 K. The wells contained 700 µl of the precipitant solution and the droplets were composed of 2 µl of the reservoir solution plus 2 µl of the protein solution at various concentrations. The first set of drops was prepared at 15 mg ml⁻¹ (prior to mixing); however, the protein was shown to be very soluble and the screens were thus repeated with increased concentrations of MsrA up to 50 mg ml⁻¹.

Five different conditions were found, producing three different crystal forms. The crystals were grown from 4–8 µl droplets composed of equal volumes of protein and precipitant solutions as described in Table 1 and equilibrated against 700 µl reservoirs at 277 K.

These conditions were strictly applied to [SeMet]-MsrA and gave exactly the same results, with no need for further optimization.

2.3. MsrA crystal X-ray characterization and data collection

X-ray diffraction experiments were performed either at 277 or 100 K. In the first case, crystals were mounted in 0.7 mm diameter glass capillaries. In the second case, crystals were taken from droplets with home-made cryo-loops and were soaked in cryoprotective solutions as described in Table 1. Cryocooling was performed by rapid immersion of crystals either in a

nitrogen-gas stream at 100 K or in liquid-nitrogen-cooled liquid ethane and then in liquid nitrogen. Preliminary diffraction patterns were measured using X-rays generated by a rotating-anode generator operating at 45 kV and 90 mA and were collected on a DIP2030 image plate (Enraf-Nonius). Complete data sets for the tetragonal crystals were collected using the same device or using synchrotron radiation on W32 beamline at LURE. Data from the hexagonal crystals were measured on the BM30 beamline at the ESRF using a MAR Research 345 image-plate detector. In all cases, *DENZO* and *SCALEPACK* (Otwinowski & Minor, 1997) were used to process and scale the raw data. Details of the final data set are given in Table 2.

2.4. [SeMet]-MsrA MAD measurements

MAD measurements were performed on hexagonal crystals of approximate dimensions 600 × 160 × 160 µm cryocooled in the same way as the native crystals (see §2.3). Two different experiments were carried out, one on beamline BM14 at the ESRF (referred to as MAD1) and the second on beamline X31 at DESY (referred to as MAD2). In each case, three different wavelengths were chosen from the inspection of the fluorescence spectrum, corresponding to the inflection point, peak and high-energy remote of the selenium *K* edge. The data sets were processed using *DENZO* (Otwinowski & Minor, 1997) and were scaled using *SCALA* (Collaborative Computational Project, Number 4, 1994) (MAD1) or *SCALEPACK* (Otwinowski & Minor, 1997) (MAD2). Further details are given in Table 3.

3. Results and discussion

Crystallization trials using standard screens have produced two families of conditions. Using salts as precipitants resulted in tetragonal crystals which grew very quickly (Table 1 and Fig. 1). Large dimensions (800 × 600 × 600 µm) were commonly obtained. Unfortunately, whatever the X-ray intensity, the temperature during X-ray exposure (100 or 277 K) and, where relevant, the nature of cryoprotectants and the manner of freezing, these tetragonal crystals diffracted poorly to 3 Å resolution on beamline W32 at LURE. Furthermore, the number of molecules in the asymmetric unit is high, a solvent content of 50% corresponding to ten molecules (5–15 if extreme solvent contents are considered). The non-

Table 3
MAD data-set statistics.

Values in parentheses refer to data in the highest resolution shell.

	Wavelength (Å)	Resolution (Å)	No. of measured reflections	No. of unique reflections	Completeness (%)	R_{sym}	I/σ_I	
MAD1	λ_1	0.9794	24.7–3.0 (3.16–3.0)	132762	36267	98.1 (93.5)	3.4 (6.7)	15.9
(ESRF, BM14)	λ_2	0.9792	24.7–3.0 (3.16–3.0)	136208	36322	98.2 (94.2)	3.4 (6.9)	14.9
	λ_3	0.9724	24.7–3.0 (3.16–3.0)	137140	36414	98.4 (96.0)	3.8 (6.5)	13.7
MAD2	λ_1	0.9797	20.0–3.0 (3.11–3.0)	194294	33121	99.3 (99.1)	3.9 (6.2)	21.1
(DESY, X31)	λ_2	0.9793	20.0–3.0 (3.11–3.0)	192813	33133	99.3 (99.0)	3.9 (6.2)	18.3
	λ_3	0.9200	20.0–3.0 (3.11–3.0)	165328	33957	98.2 (98.7)	3.8 (6.0)	23.3

crystallographic symmetry was impossible to determine, as the self-rotation function calculated with intense complete data sets only displayed a weak uninterpretable signal whatever resolution shell was used. All

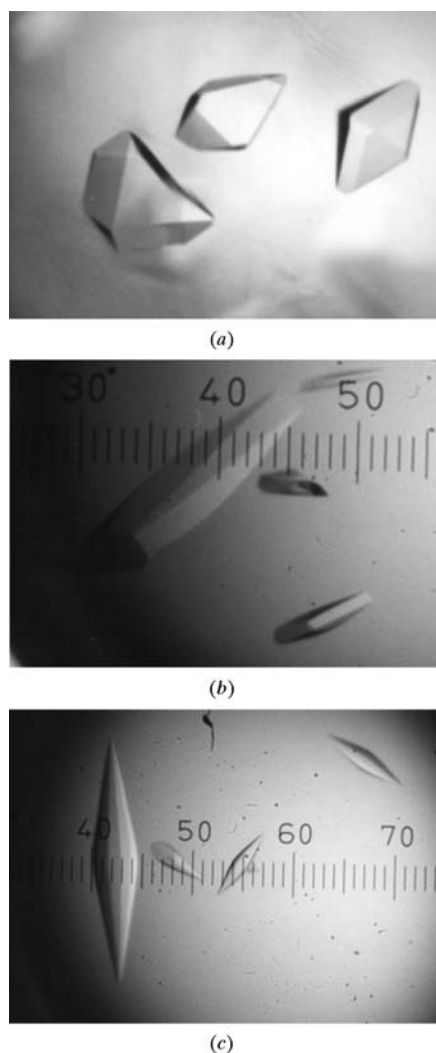


Figure 1
MsrA crystals. Approximate sizes are indicated in parentheses. (a) Tetragonal crystals obtained using condition (i) described in Table 1 (330 × 250 × 250 μm). (b) Orthorhombic crystals (680 × 220 × 120 μm). (c) Hexagonal crystals (1000 × 200 × 200 μm).

attempts to improve crystal quality remained unsuccessful. Therefore, these crystals were not used for structure determination.

The second family of conditions used PEG as a precipitant. The initial solution gave small crystals after six months; two additional months were needed to achieve dimensions of 100 μm. Searches to improve the nucleation waiting period showed that pH 6.5 to be the frontier between two crystal forms. After refinement, orthorhombic and hexagonal crystals were obtained (Table 1 and Fig. 1). The orthorhombic crystals grew faster and to larger sizes than the hexagonal ones, but they diffracted poorly and had a large calculated number of molecules in their asymmetric unit. The hexagonal crystals usually reached 600 μm in length but only 120 μm in width (maximum 200 μm) over a six-week period. These showed diffraction to 1.8 Å; a data set to 1.9 Å was collected on beamline BM30 at the ESRF (Table 2). On the basis of solvent-content evaluation, these crystals could contain two to five molecules per asymmetric unit. Calculation of the self-rotation function revealed the absence of non-crystallographic symmetry described by n -fold rotation axes relating these different molecules. In the light of the Se-atom positions (see below), further analyses confirmed that the non-crystallographic symmetry is described by axes without any particular κ -angle values corresponding to n -fold rotations. Their very weak signal compared with the level of the numerous peaks corresponding to the crystallographic operators precluded their identification.

The X-ray fluorescence spectrum from the selenomethionine-containing crystals showed an intense signal but indicated partial oxidation of some of the selenomethionine residues (Smith & Thompson, 1998). All data collected from [SeMet]-MsrA crystals have similar qualities. Data sets are at least 98.1% complete at 3 Å resolution and R_{sym} is less than 3.9%

(Table 3). Searches for the position of a maximum of 20 Se atoms were performed from one or three wavelengths, using *CNS* (Brunger *et al.*, 1998) for both MAD experiments and *SnB* (Miller *et al.*, 1994) for the MAD1 experiment. In all cases, the same 20 sites were obtained. After refinement using *MLPHARE* (Otwinowski, 1991) and the MAD1 data sets, 18 selenium sites corresponding to three molecules (six expected selenomethionine residues per molecule) were retained for electron-density calculation. This MAD-phased map is of excellent quality, showing clear protein-solvent boundaries. Model building is under way.

We are very grateful to Paul Tucker at EMBL/DESY (beamline X31), Hamburg and to the staff of beamlines BM14 and BM30 at the ESRF for their kind assistance during data collections. We thank Alain Van Dorsselaer and his collaborators for determining the molecular weights of MsrA and [SeMet]-MsrA. This research was supported by the Centre National de la Recherche Scientifique, the University Henri Poincaré-Nancy I, the FR42 Protéines, the Association de Recherche contre le Cancer (contract No. 5436) and the EU TMR/LSF grant (contract No. ERBFMGECT980134).

References

- Brot, N., Weissbach, L., Werth, J. & Weissbach, H. (1981). *Proc. Natl Acad. Sci. USA*, **78**, 2155–2158.
- Brunger, A. T., Adams, P. D., Clore, G. M., DeLano, W. L., Gros, P., Grosse-Kunstleve, R. W., Jiang, J.-S., Kuszewski, J., Nilges, M., Pannu, N. S., Read, R. J., Rice, L. M., Simonson, T. & Warren, G. L. (1998). *Acta Cryst.* **D54**, 905–921.
- Ciorba, M. A., Heinemann, S. H., Weissbach, H., Brot, N. & Hoshi, T. (1997). *Proc. Natl Acad. Sci. USA*, **94**, 9932–9937.
- Collaborative Computational Project, Number 4 (1994). *Acta Cryst.* **D50**, 760–763.
- Cudney, R., Patel, S., Weisgraber, K., Newhouse, Y. & McPherson, A. (1994). *Acta Cryst.* **D50**, 414–423.
- El Hassouni, M., Chambost, J. P., Expert, D., Van Gijsegem, F. & Barras, F. (1999). *Biochemistry*, **96**, 887–892.
- Evans, G. (1994). PhD thesis. University of Warwick, England.
- Jancarik, J. & Kim, S.-H. (1991). *J. Appl. Cryst.* **24**, 409–411.
- Levine, R. L., Berlett, B. S., Moskovitz, J., Mosoni, L. & Stadtman, E. R. (1999). *Mech. Ageing Dev.* **107**, 323–332.
- Lowther, W. T., Brot, N., Weissbach, H., Honek, J. F. & Matthews, B. W. (2000). *Proc. Natl Acad. Sci. USA*, **97**, 6463–6468.

- Matthews, B. W. (1968). *J. Mol. Biol.* **33**, 491–497.
- Miller, R., Gallo, S. M., Khalak, H. G. & Weeks, C. W. (1994). *J. Appl. Cryst.* **27**, 613–621.
- Moskovitz, J., Berlett, B. S., Poston, J. M. & Stadtman, E. R. (1997). *Proc. Natl Acad. Sci. USA*, **94**, 9585–9589.
- Moskovitz, J., Berlett, B. S., Poston, J. M. & Stadtman, E. R. (1999). *Methods Enzymol.* **300**, 239–244.
- Moskovitz, J., Poston, J. M., Berlett, B. S., Nosworthy, N. J., Szczepanowski, R. & Stadtman, E. R. (2000). *J. Biol. Chem.* **275**, 14167–14172.
- Otwinowski, Z. (1991). *Proceedings of the CCP4 Study Weekend. Isomorphous Replacement and Anomalous Scattering*, edited by W. Wolf, P. R. Evans & A. G. W. Leslie, pp. 80–86. Warrington: Daresbury Laboratory.
- Otwinowski, Z. & Minor, W. (1997). *Methods Enzymol.* **276**, 307–326.
- Ramakrishnan, V., Finch, J. T., Graziano, V., Lee, P. L. & Sweet, R. M. (1993). *Nature (London)*, **362**, 219–223.
- Sigalov, A. B. & Stern, L. J. (1998). *FEBS Lett.* **433**, 196–200.
- Smith, J. L. & Thompson, A. (1998). *Structure*, **6**, 815–819.
- Sun, H., Gao J., Ferrington, D. A., Biesada, H., Williams, T. D. & Squier, T. C. (1999). *Biochemistry*, **38**, 105–112.
- Vogt, W. (1995). *Free Radic. Biol. Med.* **18**, 93–105.